

Implementation of the modified compression field theory in a tangent stiffness-based finite element formulation

Wilkins Aquino[†] and Ibrahim Erdem

School of Civil and Environmental Engineering, Cornell University, Ithaca, NY 14853, USA

(Received July 8, 2006, Accepted January 17, 2007)

Abstract. A finite element implementation of the modified compression field theory (MCFT) using a tangential formulation is presented in this work. Previous work reported on implementations of MCFT has concentrated mainly on secant formulations. This work describes details of the implementation of a modular algorithmic structure of a reinforced concrete constitutive model in nonlinear finite element schemes that use a Jacobian matrix in the solution of the nonlinear system of algebraic equations. The implementation was verified and validated using experimental and analytical data reported in the literature. The developed algorithm, which converges accurately and quickly, can be easily implemented in any finite element code.

Keywords: finite elements; reinforced concrete; compression field theory; nonlinear analysis; shear.

1. Introduction

The finite element method is the most widely used numerical tool for analyzing complex reinforced concrete structures such as tanks, offshore structures, curved bridges, shear walls with irregularities, etc. In order to analyze such structures, robust material models for the finite element models are essential. Many different concrete material models have been reported in the literature. Material models for finite element analysis are formulated depending on the type of application and range from simple linear elastic to complex viscoplastic-damage models (Imran and Pantazopoulou 2001, Lee and Fenves 1998, 2001, Vecchio and Collins 1986, Vecchio 1989, Vecchio and Selby 1991, Vecchio 1992, Polak and Vecchio 1993, Palermo and Vecchio 2005, Zhou and Vecchio 2005, Hsu 1991, Pang and Hsu 1995, Belarbi and Hsu 1995, Pang and Hsu 1996, Hsu and Zhang 1997, Wang and Hsu 2001). Although the theory of plasticity is very suitable for calculating the limit capacity of a member and modeling path-dependent behavior of concrete, oftentimes models based on this theory may need a large number of parameters without clear physical significance and that are difficult to obtain. In many practical situations, it is of interest to estimate the monotonic nonlinear behavior of reinforced concrete structures. For this cases, theories such as rotating and fixed crack models such as the modified compression field theory (MCFT) by Vecchio and Collins (1986), and the fixed-angle softened-truss model (FA-STM) by Hsu and Zhang (1997, 2001) present attractive alternatives because of their simplicity in implementation and ease of use.

The implementation of MCFT has been addressed in secant finite element formulations by Vecchio

[†]Corresponding Author, E-mail: wa27@cornell.edu

(1990). Its implementation in tangent stiffness-based formulations has been reported too (Stevens *et al.* 1991, Cook and Mitchell 1988). However, for the solution of each load increment, they had to use the modified Newton technique to achieve convergence and they had to modify the concrete constitutive relationships to avoid sharp changes, which may prevent convergence. More robust implementations of MCFT have not been reported in the literature to the best knowledge of the authors. Many available commercial and in-house finite element codes use tangential formulations to solve the nonlinear system of equations arising from the finite element discretization. This formulation requires the calculation of a material tangent stiffness matrix from the constitutive model during the iterative solution process, which may not be a trivial step in many circumstances.

In this paper, a detailed, more robust implementation of MCFT in a tangent stiffness-based finite element scheme is presented. First, the fundamental concepts from MCFT are described. Then, the finite element formulation is presented, addressing the issues of stress updating and computing the tangent stiffness matrix from the material model. The different components of a reinforced concrete material model based on MCFT are explained followed by numerical examples and the validation of the implementation.

2. The modified compression field theory (MCFT)

MCFT was introduced by Vecchio and Collins (1986) and it was developed from the original compression field theory developed by Mitchell and Collins (1974). In these theories, relationships between average stresses and strains were postulated based on experimental observations. Cracks in these theories are treated in a distributed sense.

The following are the assumptions made in MCFT.

- There is a one-to-one correspondence between stresses and strains. That is, the model is non-linear elastic.
- Average stress and strain are defined for areas which are large enough to cover several cracks.
- There is perfect bonding between reinforcing bars and concrete (i.e. no slip).
- The longitudinal and transverse reinforcing bars are uniformly distributed.
- The principal strain directions are coincident with the principal stress directions.

Three main components define MCFT: equilibrium equations, constitutive relationships, and load transmission conditions at cracks. These components are extensively described in Vecchio and Collins (1986) and are briefly outlined herein for completeness.

2.1 Constitutive relationships in MCFT

The constitutive relationships involved in MCFT are presented in principal stress-strain space. Vecchio and Collins (1986) reported that the principal compressive stress at a point in concrete depends on both the principal tensile and compressive strains, while the principal tensile stress is only dependent on the principal tensile strain (i.e. decoupled from the compressive strain).

The compressive stress is calculated in MCFT as

$$\sigma_{c2} = \sigma_{c2\max} \left[2 \frac{\varepsilon_{c2}}{\varepsilon_o} - \left(\frac{\varepsilon_{c2}}{\varepsilon_o} \right)^2 \right] \quad (1)$$

where σ_{c2} is the minimum principal stress (compression in MCFT), ε_o is the strain at the peak stress in a

uniaxial compression test, and ε_{c2} is the minimum principal strain. The factor $\sigma_{c2\max}$ accounts for the state of biaxial tension-compression and is calculated as

$$\sigma_{c2\max} = \frac{f'_c}{0.8 - 0.34 \frac{\varepsilon_{c1}}{\varepsilon_o}} \quad (2)$$

where f'_c is the uniaxial compressive strength of the concrete.

The stress-strain curve of concrete under tension is defined as linear elastic up to cracking as

$$\sigma_{c1} = E_c \varepsilon_{c1} \quad (3)$$

where E_c is the modulus of elasticity of concrete, σ_{c1} is the maximum principal tensile stress, and ε_{c1} is the maximum principal strain. After cracking, the tensile stress in the concrete is taken as

$$\sigma_{c1} = \frac{f_{cr}}{1 + \sqrt{500 \cdot \varepsilon_{c1}}} \quad (4)$$

The stress-strain behavior of the steel is assumed to be elastic-perfectly plastic in this work. That is, the material is assumed to be linearly elastic up to yielding and then remain at the yield stress for strains greater than the yield strain.

2.2 Equilibrium equations

Equilibrium equations are used to calculate the average stresses at a point from the concrete and steel contributions as

$$\begin{aligned} \sigma_x &= \sigma_{cx} + \rho_{sx} \cdot \sigma_{sx} \\ \sigma_y &= \sigma_{cy} + \rho_{sy} \cdot \sigma_{sy} \\ \sigma_{xy} &= \sigma_{cxy} \end{aligned} \quad (5)$$

where σ_x , σ_y , and σ_{xy} are the average stress in the X-direction, average stress in the Y-direction, and average shear stress calculated at a material point in reinforced concrete. The quantities σ_{cx} and σ_{cy} represent axial stresses in the concrete, while σ_{sx} and σ_{sy} represent axial stresses in the steel. Neglecting the average shear stress contribution of the steel, the shear stress σ_{xy} is assumed to be equal to the shear stress carried by the concrete, σ_{cxy} . Reinforcement ratios in the X and Y directions are represented by ρ_{sx} and ρ_{sy} , respectively. These ratios are given as cross sectional area of steel to area of concrete.

2.3 Load transmission conditions at cracks

The stress-strain relationships described above are valid in an average sense. However, stresses in the steel at cracks will be higher than their average values. Therefore, it is necessary to ensure that the steel reinforcement is capable of transmitting the demanded average tension stresses across cracks.

Vecchio and Collins (1986) derived the following conditions which are used to ensure that enough

capacity exists in the concrete and steel to properly transmit tension across cracks.

$$\begin{aligned}\sigma_{sxcr} &= \sigma_{sx} + (\sigma_{c1} + \sigma_{ci} + v_{ci}/\tan\theta)/\rho_{sx} \leq \sigma_{yx}^{yield} \\ \sigma_{sy-cr} &= \sigma_{sy} + (\sigma_{c1} + \sigma_{ci} - v_{ci}/\tan\theta)/\rho_{sy} \leq \sigma_{yy}^{yield}\end{aligned}\quad (6)$$

In the above equations, σ_{sxcr} and σ_{sy-cr} are the axial stresses in the steel in the X and Y directions at the crack face, respectively, σ_{xx}^{yield} is the yield stress of the steel in the X direction, σ_{yy}^{yield} is the yield stress of the steel in the Y direction, σ_{ci} is the compressive stress acting on the crack, v_{ci} is the shear stress acting along the crack, θ is the angle of inclination of cracks with respect to the X-axis.

The maximum shear that can act along the crack is calculated as Vecchio and Collins (1986)

$$v_{ci\max} = \frac{\sqrt{-f'_c}}{0.31 + 24 \cdot w/(a + 16)} \quad (7)$$

Where w is the estimated crack width, a is the maximum aggregate size. The crack width, w , is calculated as

$$w = \varepsilon_c s_\theta \quad (8)$$

The spacing of the cracks along the principal direction tensile direction, s_θ , can be calculated from the spacing of the cracks perpendicular to the reinforcement in X-direction and Y-direction as

$$s_\theta = \frac{1}{\frac{\sin\theta}{s_{mx}} + \frac{\cos\theta}{s_{my}}} \quad (9)$$

where s_{mx} and s_{my} are the average spacing of the cracks perpendicular to the X and Y directions, respectively.

3. Implementation of MCFT in finite element analysis

This section describes how MCFT can be implemented in a displacement-based finite element formulation that uses a tangent stiffness matrix. The crucial aspects for this implementation are how stresses are updated and how the material tangent stiffness is computed at integration points in iterative incremental solution schemes. Only material nonlinearity is considered herein.

3.1 Finite element formulation of the nonlinear problem

The principle of virtual work is commonly used to derive the finite element formulation of nonlinear stress analysis problems. The principle of virtual work can be expressed as

$$\int_{\Omega} \{\delta\varepsilon\}^T \{\sigma\} d\Omega = \int_{\Gamma} \{\delta u\}^T \{\tau\} d\Gamma + \int_{\Omega} \{\delta u\}^T \{b\} d\Omega + \sum_i P_i \delta u_i \quad (10)$$

Implementation of the modified compression field theory in a tangent stiffness-based finite element formulation

where $\{\delta u\}$ is an admissible virtual displacement field in the domain Ω and its boundary Γ , $\{\delta \varepsilon\}$ is the corresponding virtual strain field, $\{\sigma\}$ is the stress vector, $\{\tau\}$ represents the tractions applied over part of the boundary, $\{b\}$ represents body forces, and P_i are applied point forces.

If the domain Ω is divided into n finite elements and for each element, the displacement vector $\{u\}$ and virtual displacement vector $\{\delta u\}$ are related to the nodal displacements of the element $\{u^e\}$ with the same interpolation functions $[N]$, one can obtain the following from Eq. (10):

$$\{\delta U\}^T \left[\sum_{elements} \int_{\Omega_e} [B]^T \{\sigma\} d\Omega^e - \{Q\} \right] = 0 \quad (11)$$

where $[B]$ is the matrix representing the partial derivatives of the shape functions with respect to position. $\{\delta U\}$ is the virtual displacement vector containing all degrees-of-freedom in the domain, $\{Q\}$ is the external load vector defined as

$$\{Q\} = \sum_{elements} \left(\int_{\Gamma^e} [N]^T \{\tau\} d\Gamma^e + \int_{\Omega^e} [N]^T \{b\} d\Omega^e \right) + \{P_{po \text{ int}}\} \quad (12)$$

and $\{P_{po \text{ int}}\}$ is a vector of point loads.

Since Eq. (11) must hold for all choices of $\{\delta U\}$, then the expression in the square brackets must vanish. Then,

$$\sum_{elements} \int_{\Omega_e} [B]^T \{\sigma\} d\Omega^e = \{Q\} \quad (13)$$

If the left hand side of Eq. (13) is defined as the internal force resisting vector, $\{I\}$, then the system of equations for a non linear problem can be rewritten as,

$$\{Q\} - \{I\} = 0 \quad (14)$$

The Newton-Raphson or modified Riks methods (Bathe 1996, Crisfield 1991, Belytschko *et al.* 2000) are commonly used to solve the system of equations described in Eq. (14). These iterative solution procedures require the calculation of a tangent stiffness or Jacobian matrix defined as

$$[K_T] = \left[\frac{\partial \{I\}}{\partial \{U\}} \right] \quad (15)$$

The global Jacobian matrix is assembled from the contributions of the local material tangent stiffness as

$$[K_T] = \sum_{elem \Omega_e} \int [B]^T [D] [B] d\Omega \quad (16)$$

where the local material tangent stiffness has been defined as

$$[D] = \frac{\partial \{\sigma\}}{\partial \{\varepsilon\}} \quad (17)$$

The main tasks that need to be performed by the constitutive model implementation in the finite element scheme shown above are updating the stresses to compute the internal force resisting vector using internal force resisting vector, $\{I\}$ and computing the material tangent stiffness matrix using Eq. (17). These quantities are computed at each Gauss integration point in the finite element mesh. The calculation of a Jacobian matrix is many times a non-trivial task. This is the case in MCFT mainly because of the need to check for load transmission conditions at cracks.

3.2 Implementation of MCFT in a finite element scheme

This section shows how the equations of MCFT enter the finite element formulation described above. The algorithm, implemented using FORTRAN 77, is composed of two main parts: stress updating and computation of the material Jacobian matrix.

The layout of the reinforced concrete model implementation is shown in Fig. 1. The main finite element program supplies the material model subroutine with strains at integration points for computing stresses and the material Jacobian matrix. Stress updating occurs separately for steel and concrete and these tasks are implemented as separate subroutines. Similarly, the steel and concrete contributions to the Jacobian matrix are computed in a separate subroutine. Box 1 shows the organization of the reinforced concrete material subroutine.

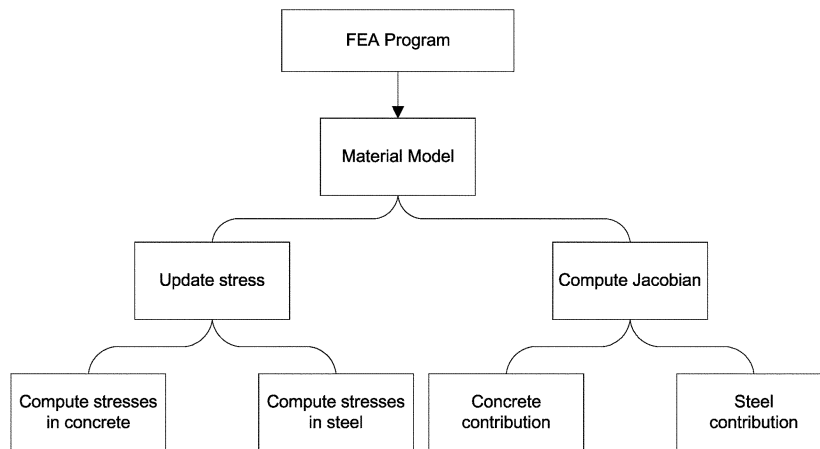


Fig. 1 Layout of a reinforced concrete material model implementation

```

RC Material Subroutine
  Call Steel Stress Subroutine
  Call Concrete Stress Subroutine
  Compute total stress from steel and
  concrete stress contributions using Eq. (5)
  Call Jacobian matrix Subroutine
  Return updated stresses and Jacobian Matrix
End RC Material Subroutine
  
```

Box 1 Reinforced concrete material subroutine

```

Steel Stress Update Subroutine
*Elastic-perfectly plastic*
If strain component < yield strain
     $\sigma_{xx} = E\varepsilon_{xx}$ 
or
     $\sigma_{yy} = E\varepsilon_{yy}$ 
Else
     $\sigma_{xx} = \sigma_{xx}^{yield}$ 
or
     $\sigma_{yy} = \sigma_{yy}^{yield}$ 
end If
Return steel stresses
End Steel Stress Subroutine
    
```

Box 2 Steel stress subroutine

3.2.1 Main material model subroutine

Steel and concrete stresses are computed in separate subroutines called by the RC Material Subroutine. The steps involved in this process are described in Box 1. The implementation in this paper assumes that bars are oriented in the global X and Y directions. If bars with arbitrary orientations are used, Eqs. (5) and (6) must be modified to take directionality of steel into account.

Steel stresses are computed as shown in Box 2. This implementation assumes elastic-perfectly plastic behavior of the steel. More sophisticated steel models that take strain hardening into consideration can also be similarly implemented.

3.2.2 Concrete stress subroutine

Concrete behavior is described using three different states of stress: biaxial compression, biaxial tension, and biaxial tension-compression. In all three cases, the stress state is determined in the principal stress/strain space. Therefore, only principal strains are computed and used to determine principal stresses. Once

```

Concrete Stress Subroutine
Compute principal strains  $\varepsilon_1$  and  $\varepsilon_2$ 
Compute principal plane angle  $\theta$ 
If  $\varepsilon_1$  and  $\varepsilon_2$  are both positive or negative
    Call Biaxial Stress Subroutine
Else
    Call MCFT Subroutine
End If
Compute concrete average stresses by
transforming principal stresses back to
original coordinate system
Return concrete average stresses
End Concrete Stress Subroutine
    
```

Box 3 Concrete stress subroutine

principal stresses are determined, they are transformed back to the original coordinate system and passed back to the main material subroutine.

The subroutine for computing concrete stresses is described in Box 3. Once principal strains are computed, the state of stress (i.e. biaxial compression, biaxial tension, or tension compression) is inferred from the signs of the principal strains. Principal strains are sent to different subroutines depending on the stress state for computing principal stresses.

3.2.3 Biaxial stress subroutine

The structure of the biaxial stress subroutine is illustrated in Box 4. If both principal strains are positive, then a state of biaxial tension exists. For this case, the stress-strain behavior is assumed to be uniaxial in each direction. Principal stresses are computed separately from strains for each axis using Eqs. (3) and (4).

If both strains are negative, the material point is in a state of biaxial compression. The implementation given in this paper uses the equations described in Vecchio (1992). These equations are given as

$$K_1 = 1 - 0.92 \left(\frac{\sigma_2}{f'_c} \right) - 0.76 \left(\frac{\sigma_2}{f'_c} \right)^2$$

$$\sigma_{p1} = K_1 f'_c$$

$$\varepsilon_{p1} = K_1 \varepsilon'_{co}$$

```

Biaxial Stress Subroutine
  *Biaxial tension*
  If  $\varepsilon_1$  and  $\varepsilon_2 > 0$ 
    Compute  $\sigma_1$  using Eqs. (3) and (4)
  Else
    *Biaxial compression*
    Initialize  $\sigma_1 = \sigma_2 = 0$ 
     $i = 1$ 
    Norm( $i$ ) = 0
    Error = 9999
    Do while Error < tolerance and  $i < \text{Max iterations}$ 
      Compute  $K_1$  and  $K_2$  as shown in Eqs. (21)
      Compute
         $\varepsilon_{1p} = K_1 \varepsilon_{co}$ 
         $\varepsilon_{2p} = K_2 \varepsilon_{co}$ 
      Compute  $\sigma_1$  and  $\sigma_2$  as shown in Eqs. (21)
      norm( $i+1$ ) =  $\sqrt{\sigma_1^2 + \sigma_2^2}$ 
      Error = |norm( $i$ ) - norm( $i+1$ )|
      increment  $i$ 
    end Do while
  End If
End Biaxial Stress Subroutine

```

Box 4 Biaxial stress subroutine

$$\begin{aligned}\sigma_1 &= -\sigma_{p1} \left[2 \left(\frac{\varepsilon_1}{\varepsilon_{p1}} \right) - \left(\frac{\varepsilon_1}{\varepsilon_{p1}} \right)^2 \right], 0 > \varepsilon_1 > \varepsilon_{p1} \\ \sigma_1 &= -\sigma_{p1} \left[1 - \left(\frac{\varepsilon_1 - \varepsilon_{p1}}{2 \varepsilon_{co} - \varepsilon_{p1}} \right)^2 \right], \varepsilon_{p1} > \varepsilon_1 > -2 \varepsilon_{co}\end{aligned}\quad (18)$$

The same procedure is used for computing σ_2 , but the roles of σ_1 and σ_2 in Eq. (18) are reversed. Notice that the above system of equations is nonlinear, so it needs to be solved iteratively as shown in Box 4. The direct substitution method shown in Box 4 produced fast convergence for the examples investigated in this research. Other solution methods for nonlinear algebraic equations such as the Newton-Raphson scheme can also be used.

3.2.4 Modified compression field theory (MCFT) subroutine

MCFT is used to determine the stress state when biaxial tension-compression stress states exist as illustrated in Box 5. The compressive and tensile stresses σ_2 and σ_1 , respectively, are determined using the principal strains and Eqs. (1)-(4).

A fundamental aspect of MCFT is that the tension field transmitted across cracks is limited by two main criteria: yielding of reinforcement crossing a crack and the maximum shear stress that can be carried at the surface of a crack. The admissible tension field conditions across the cracks are checked using Eqs. (6)-(9). The implementation of the enforcement of these conditions is shown in Box 5. Notice that θ represents the crack orientation, while ϕ represents the principal direction angle (Vecchio and Collins 1986).

The first condition considers yielding of the reinforcement at the crack in the X-direction, while the reinforcement in the Y-direction remains below its yield limit. The shear stress, v_{ci} , needed to sustain the average tensile stress, σ_1 , is computed using the first Equation in (6). If the maximum shear stress admissible at a crack, $v_{ci\max}$, is exceeded, then a new tensile stress, $^1\sigma_1$, is calculated so that $v_{ci} = v_{ci\max}$. The same procedure is repeated for a second condition in which the steel in the Y-direction reaches yielding at the crack face, while the steel in the X-direction remains below its yield point. If the maximum shear is exceeded, a new admissible tensile stress, $^2\sigma_1$, is computed in order to maintain the shear stress at the crack below its maximum value. The third condition computes the maximum tensile stress, $^3\sigma_1$, that can be developed when the reinforcement in the X and Y directions reaches its yield limit. Finally, the average concrete tensile stress selected is the minimum of the above four possible choices (σ_1 , $^1\sigma_1$, $^2\sigma_1$, and $^3\sigma_1$).

3.2.5 Jacobian matrix subroutine

Once the stresses are updated, the material stiffness or Jacobian matrix needs to be determined as explained previously. The material stiffness matrix in Eq. (17) involves the derivative of the stresses with respect to the strains. Although closed-form expressions for the concrete Jacobian matrix can be calculated using the stress-strain relationships described in this paper, the resulting expressions are cumbersome and their implementation is lengthy, increasing the possibilities of introducing errors in the code. A simpler approach is to use a finite difference approximation of the material Jacobian matrix. Because of the modular structure of this implementation, the process of computing this finite approximation is fairly simple as illustrated in Box 6. The computational cost of following this approach proved to be low in comparison with the benefits of code simplicity.

Concrete MCFT Subroutine

Compute σ_1 and σ_2 using Eqs.(1)-(4)

Check if maximum shear stress at cracks is not exceeded as follows. Neglect compressive stress across cracks

Compute crack angle θ

If ε_1 and $\varepsilon_2 \neq 0$

$$\theta = \phi - \frac{\pi}{2}$$

Else

$$\theta = \phi$$

End if

Compute $\omega, s_\theta, v_{ci\max}$ using Eqs. (7)-(9)

* First check: use equilibrium in X-direction in Eq. (6)*

Compute $v_{ci} = [\rho_x(\sigma_{xx}^{yield} - \sigma_{xx}) - \sigma_{c1}] \tan(\theta)$

If $|v_{ci}| > v_{ci\max}$

$$^1\sigma_1 = \rho_x(\sigma_{xx}^{yield} - \sigma_{xx}) \pm \frac{v_{ci\max}}{\tan(\theta)}$$

End If

* Second check: use equilibrium in Y-direction in Eq. (6)*

Compute $v_{ci} = \frac{[\sigma_1 - \rho_y(\sigma_{yy}^{yield} - \sigma_{yy})]}{\tan(\theta)}$

If $|v_{ci}| > v_{ci\max}$

$$^2\sigma_1 = \rho_y(\sigma_{yy}^{yield} - \sigma_{yy}) \mp v_{ci\max} \tan(\theta)$$

End If

Third check: verify that reinforcement does not yield in X and Y directions simultaneously

$$^3\sigma_1 = \rho_x(\sigma_{xx}^{yield} - \sigma_{xx}) \sin^2(\theta) + \rho_y(\sigma_{yy}^{yield} - \sigma_{yy}) \cos^2(\theta)$$

Select admissible tensile stress across cracks

$$\sigma_1 = \min(\sigma_1, ^1\sigma_1, ^2\sigma_1, ^3\sigma_1)$$

End Concrete MCFT Subroutine

Box 5 Concrete MCFT subroutine

To compute the concrete contribution of the material Jacobian matrix, first an increment of strain is defined as shown in Box 6. Then, forward and backward strain steps are created using this increment of strain. The Jacobian matrix is formed column by column, as shown in Box 6, by progressive calls to the concrete stress update subroutine using the incremented strains. The steel contribution can be easily computed in closed form as shown in Box 6. The total material stiffness matrix is then formed by adding the concrete and the steel contributions.

It is important to realize that the Jacobian matrix computed using the above procedure will be in general non-symmetric. Therefore, it is important to bear this in mind when invoking solvers that may try to

Jacobian Subroutine

Define a small strain increment $\delta\varepsilon = \frac{\varepsilon_{co}}{1000}$

Compute incremented strains

$$\begin{aligned} \left\{ \begin{matrix} {}^1\varepsilon_{incx} \end{matrix} \right\} &= \begin{Bmatrix} \varepsilon_{xx} + \delta\varepsilon \\ \varepsilon_{yy} \\ \varepsilon_{xy} \end{Bmatrix} \\ \left\{ \begin{matrix} {}^2\varepsilon_{incx} \end{matrix} \right\} &= \begin{Bmatrix} \varepsilon_{xx} - \delta\varepsilon \\ \varepsilon_{yy} \\ \varepsilon_{xy} \end{Bmatrix} \end{aligned}$$

Compute stresses using above strains from Concrete Stress Subroutine

$\left\{ \begin{matrix} {}^1\sigma_{incx} \end{matrix} \right\} = \text{Call Concrete Stress Subroutine}(\left\{ \begin{matrix} {}^1\varepsilon_{incx} \end{matrix} \right\})$

$\left\{ \begin{matrix} {}^2\sigma_{incx} \end{matrix} \right\} = \text{Call Concrete Stress Subroutine}(\left\{ \begin{matrix} {}^2\varepsilon_{incx} \end{matrix} \right\})$

Compute Column 1 of Jacobian matrix

$$[D_{co}(1:3,1)] = \frac{\left\{ \begin{matrix} {}^1\sigma_{incx} & -{}^2\sigma_{incx} \end{matrix} \right\}}{2\delta\varepsilon}$$

Repeat above procedure for Columns 2 and 3.

Steel Contribution

If $\varepsilon_{xx} < \varepsilon_{xx}^{yield}$

$$E_{sx} = E_s$$

Else

$$E_{sx} = 0$$

End If

Repeat for Y component

$$[D_s] = \begin{bmatrix} \rho_x E_{sx} & 0 & 0 \\ 0 & \rho_y E_{sy} & 0 \\ 0 & 0 & 0 \end{bmatrix}$$

$$[D] = [D_{co}] + [D_s]$$

End Jacobian Subroutine

Box 6 Jacobian matrix subroutine

exploit symmetry to increase computational speed. Often finite element software use symmetric solvers by default and non-symmetric solvers have to be activated by the user.

4. Validation and verification examples

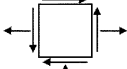
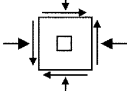
The implementation described above was incorporated into a user-defined subroutine in a tangent stiffness-based finite element code. The commercial software ABAQUS was utilized for the examples presented herein. Shear panels tested by Vecchio, Collins, and co-workers at the University of Toronto were used to validate the implementation (Vecchio and Collins 1986, Chan 1989, Bhide and Collins 1987). In addition, the results obtained with the described implementation were compared to solutions obtained with other software implementation of MCFT (Bentz 2000). Four node quadrilateral elements with full integration were used for all the analyses.

Square reinforced concrete panels with a side dimension of 890 mm were used for the validation. The thickness of the panels was 70 mm. The maximum aggregate size used for the concrete was 6 mm. The panels were reinforced with two layers of 6 mm diameter reinforcing bars in each direction and the steel had a Young's modulus of 200 GPa. Other material properties are given in Table 1.

Three different panels were investigated: two solid panels, PV20 and PB5, and one with a square opening at its center, PC5. Details of the panel geometry, reinforcement ratios, and loading conditions are also given in Table 1. Panel PV20 was loaded under pure shear, Panel PC5 was loaded under biaxial compression and shear, and Panel PB5 was loaded under biaxial tension-compression and shear. There are 289 elements in the finite element model of PV20 and PB5. The elements density around the corner of the hole in PC5 was increased, which resulted in twice the number of elements used in PV20.

Shear stress-strain response curves for panels PV20 and PB5 are shown in Fig. 2 and Fig. 3, respectively. The plots show results from laboratory experiments, the current MCFT implementation, and the software Membrane 2000 (Bentz 2000, Bentz *et al.* 2006). As can be seen from Figs. 2 and 3, the results obtained with the proposed implementation of MCFT follows closely the results obtained with Membrane 2000. In addition, the initial stiffness and initial cracking predicted by the current MCFT implementation are in close agreement with the experimental values obtained for both specimens. The predicted maximum shear stress satisfactory agrees with the experimental values in both cases, but the error was more pronounced in the case of Panel PB5. The largest discrepancy between the predicted

Table 1 Details of the test specimens

Specimen	f'_c (MPa)	ϵ_o	ρ_x (%)	σ_{xx}^{yield} (MPa)	ρ_y (%)	σ_{yy}^{yield} (MPa)	Loading σ_{xx} : σ_{yy} : σ_{xy}
PV20	19.6	0.0018	1.785	460	0.885	297	0: 0: 1 
PB5	23.5	0.0018	1.085	415	0	-	1: -1: 1 
PC5	27.3	0.0018	1.65	390	0.82	390	0.32: 0.32: 1 

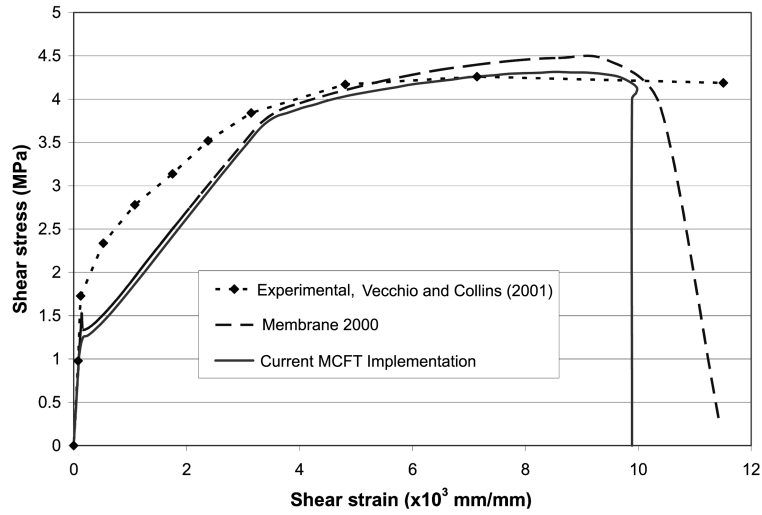


Fig. 2 Shear stress-strain behavior of Panel PV20

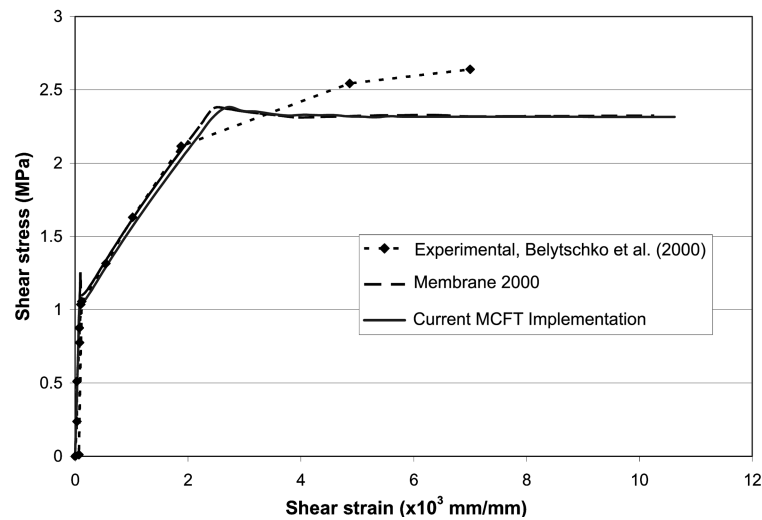


Fig. 3 Shear stress-strain behavior of Panel PB5

and the experimental responses occurred in the postpeak branch. This result was expected as the failure mechanisms that occurred in the actual panels such as slippage at cracks or localized crushing cannot be captured by MCFT.

4.1 Panel with square opening (PC5)

In order to test the performance of the current MCFT implementation with a panel structure that results in a non-uniform stress distribution, a reinforced concrete panel with a square opening at its center was analyzed. This configuration results in stress conditions that span the four states considered by the implementation: tension-tension, compression-compression, and tension-compression. The results of the

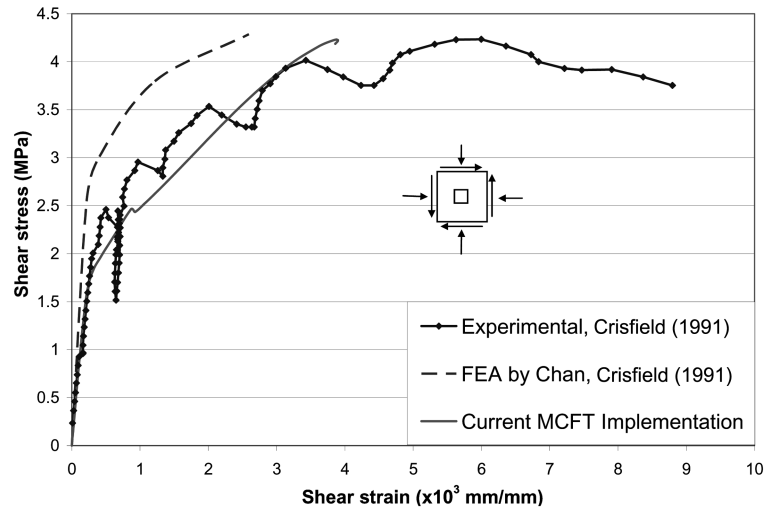


Fig. 4 Average shear stress-strain response of Panel PC5

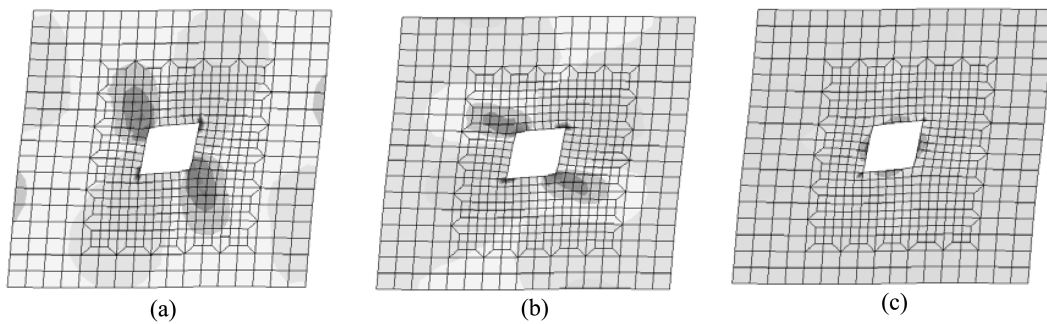


Fig. 5 (a) Axial stress in Y-direction (σ_{yy}), (b) Axial stress in X-direction (σ_{xx}), (c) Shear stress (σ_{xy})

finite element analysis were compared to experimental and numerical analysis results reported in (1989).

Fig. 4 shows plots of the average shear stress-strain behavior of Panel PC5. Fig. 5 shows the finite element mesh used for this problem and the non-uniform stress distribution that results around the opening. It can be observed in the experimental results that unloading occurred at some instances during testing. This unloading was the result of test stops for reading of the instrumentation. As can be seen from Fig. 4, the initial stiffness, cracking stress, and ultimate shear strength of the specimen were satisfactorily estimated by the current finite element implementation whereas the ultimate displacement was lower than the experimental counterpart. The finite element results reported by Chan (1989) are also shown in Fig. 4.

5. Comments on mesh objectivity

It is well known that finite element implementations of softening material behavior result in non-objective meshes. That is, results are dependent upon the mesh size used for the analysis if no steps are taken to prevent this phenomenon. Several approaches have been proposed to alleviate mesh dependency

problems such as non-local formulations, enriched interpolation functions, and the use of a characteristic element length in the constitutive models (Bazant and Cedolin 1991, Ortiz *et al.* 1987, Bontempi and Malerba 1997). The implementation of MCFT presented in this paper displays mesh dependency pathologies since no regularization was incorporated into the formulation. This can be fixed by using the approach proposed in Bazant and Cedolin (1991, Ortiz *et al.* (1987), Bontempi and Malerba (1997) in which constitutive laws are modified to incorporate a characteristic length deduced from energy constraints. This approach ensures that energy dissipation per unit volume will not depend on the element size selected.

Another approach that could be used with the implementation described in this paper is to select the size of the element to be approximately equal to the expected crack spacing. This strategy was used by the authors and produced adequate results. This spacing is consistent with the experiments from which MCFT equations were derived. The authors plan in the future to investigate different regularization schemes and their incorporation into the current MCFT implementation in order to devise a more robust strategy for alleviating mesh dependency.

6. Conclusions

In this paper, a simple implementation of the Modified Compression Field Theory (MFCT) has been presented. The algorithm can be used with any tangent stiffness-based finite element formulation. The implementation was validated using experimental data from tests performed on reinforced concrete panels. It was found that the results obtained with the current implementation of MCFT are in agreement with experimental and analytical results reported in the literature. The algorithm described in this paper was implemented using FORTRAN 77. The code is available for research and educational use from the authors.

Acknowledgements

Wilkins Aquino thanks Profs. David Pecknold and Daniel Kuchma from the University of Illinois at Urbana-Champaign (UIUC) for their thorough and caring advice on computational mechanics and the modified compression field theory, which led to this paper.

References

- Bathe, K. J. (1996), *Finite Element Procedures*, Prentice Hall.
- Bazant, Z. P. and Cedolin, L. (1991), *Stability of Structures*, Oxford University Press.
- Belarbi, A. and Hsu, T. T. C. (1995), "Constitutive laws of softened concrete in biaxial tension-compression", *ACI Struct. J.*, **92**(5), 562-573.
- Belytschko, T., Liu, W. K. and Moran, B. (2000), *Nonlinear Finite Elements for Continua and Structures*, Wiley.
- Bentz, E. C. (2000), "Sectional analysis of reinforced concrete members", Ph.D, Civil Engineering, University of Toronto, PhD, Civil Engineering, University of Toronto, Toronto, CA.
- Bentz, E. C., Vecchio, F. J. and Collins, M. P. (2006), "Simplified modified compression field theory for calculating shear strength of reinforced concrete elements", *ACI Struct. J.*, **103**(4), 614-624.
- Bhide, S. B. and Collins, M. P. (1987), *Reinforced Concrete Elements in Shear and Tension*, University of Toronto: Toronto, CA.

- Bontempi, F. and Malerba, P. G. (1997), "The role of softening in the numerical analysis of RC framed structures", *Struct. Eng. Mech.*, **5**(6), 785-801.
- Chan, C. C. L. (1989), "Testing of reinforced concrete membrane elements with perforations", M.S., Civil Engineering, University of Toronto, Toronto, CA.
- Cook, W. D. and Mitchell, D. (1988), "Studies of disturbed regions near discontinuities in reinforced concrete members", *ACI Struct. J.*, **85**(2), 207-216.
- Crisfield, M. A. (1991), *Non-Linear Finite Element Analysis of Solids and Structures*. Vol. 1. Wiley.
- Hsu, T. T. C. (1991), "Nonlinear-analysis of concrete membrane elements", *ACI Struct. J.*, **88**(5), 552-561.
- Hsu, T. T. C. and Zhang, L. X. (1997), "Nonlinear analysis of membrane elements by fixed-angle softened-truss model", *ACI Struct. J.*, **94**(5), 483-492.
- Imran, I. and Pantazopoulou, S. J. (2001), "Plasticity model for concrete under triaxial compression", *J. Eng. Mech.*, ASCE, **127**(3), 281-290.
- Lee, J. and Fenves, G. L. (2001), "A return-mapping algorithm for plastic-damage models: 3-D and plane stress formulation", *Inter. J. Numer. Methods Eng.*, **50**(2), 487-506.
- Lee, J. H. and Fenves, G. L. (1998), "Plastic-damage model for cyclic loading of concrete structures", *J. Eng. Mech.*, ASCE, **124**(8), 892-900.
- Mitchell, D. and Collins, M. P. (1974), "Diagonal compression field theory-a rational model for structural concrete in pure torsion", *ACI J.*, **71**(8), 396-408.
- Ortiz, M., Leroy, Y. and Needleman, A. (1987), "A finite-element method for localized failure analysis", *Comput. Methods Appl. Mech. Eng.*, **61**(2), 189-214.
- Palermo, D. and Vecchio, F. J. (2002), "Behavior of three-dimensional reinforced concrete shear walls", *ACI Struct. J.*, **99**(1), 81-89.
- Pang, X. B. D. and Hsu, T. T. C. (1995), "Behavior of reinforced concrete membrane elements in shear", *ACI Struct. J.*, **92**(6), 665-679.
- Pang, X. B. D. and Hsu, T. T. C. (1996), "Fixed angle softened truss model for reinforced concrete", *ACI Struct. J.*, **93**(2), 197-207.
- Polak, M. A. and Vecchio, F. J. (1993), "Nonlinear-analysis of reinforced-concrete shells", *J. Struct. Eng.*, ASCE, **119**(12), 3439-3462.
- Stevens, N. J., Uzumeri, S. M., Collins, M. P. and Will, G. T. (1991), "Constitutive model for reinforced-concrete finite-element analysis", *ACI Struct. J.*, **88**(1), 49-59.
- Vecchio, F. J. (1989), "Nonlinear finite-element analysis of reinforced-concrete membranes", *ACI Struct. J.*, **86**(1), 26-35.
- Vecchio, F. J. (1990), "Reinforced concrete membrane element formulations", *J. Struct. Eng.*, ASCE, **116**(3), 730-750.
- Vecchio, F. J. (1992), "Finite-element modeling of concrete expansion and confinement", *J. Struct. Eng.*, ASCE, **118**(9), 2390-2406.
- Vecchio, F. J. and Collins, M. P. (1986), "The modified compression-field theory for reinforced-concrete elements subjected to shear", *J. American Concrete Institute*, **83**(2), 219-231.
- Vecchio, F. J. and Selby, R. G. (1991), "Toward compression-field analysis of reinforced-concrete solids", *J. Struct. Eng.*, ASCE, **117**(6), 1740-1758.
- Wang, T. J. and Hsu, T. T. C. (2001), "Nonlinear finite element analysis of concrete structures using new constitutive models", *Compos. Struct.*, **79**(32), 2781-2791.
- Zhou, C. E. and Vecchio, F. J. (2005), "Nonlinear finite element analysis of reinforced concrete structures subjected to transient thermal loads", *Compos. Concrete*, **2**(6), 455-479.